*American Mineralogist, Volume 82, pages 1225–1240, 1997*

# Experimental study of the Fe-Mg exchange between garnet and biotite: Constraints on the mixing behavior and analysis of the cation-exchange mechanisms

**C.K. Gessmann,* B. Spiering, and M. Raith**

Mineralogisch-Petrologisches Institut, Universität Bonn, 53115, Bonn, Germany

## Abstract

New experimental data are presented for the Fe-Mg exchange between garnet and biotite in the temperature range 600–800 °C at 0.2 GPa. The Fe-Mg-Al mixing properties of biotite were evaluated and the garnet-biotite geothermometer was recalibrated. SEM observations and comparative laser granulometry show that solution-precipitation largely controls the cation exchange mechanism, involving about 50% of the mineral volume. Mass balance calculations emphasize the effectiveness of the experimental design: A high Gt/Bio ratio ensures that the garnet composition remains approximately constant and close to equilibrium, even if the entire garnet volume is not involved in the cation exchange. Progressively decreasing partition coefficients with decreasing Fe content of garnet indicate nonideal thermodynamic mixing behavior. The application of various garnet activity models support nearly ideal Fe-Mg mixing in garnet. The remaining nonidealities were attributed to nonideal Fe, Mg, and Al mixing in biotite as the initially binary biotite samples changed toward more aluminous compositions during the experiments. Adopting the standard state properties and the garnet-mixing model of Berman (1988, 1990), least square regressions reveal nearly ideal mixing of Fe and Mg in biotite with $W_{FeMg} = -2.3 \pm 1.6$ kJ/mol, while the difference between Fe-Al and Mg-Al interactions yield $\Delta W_{Al} = -17.6 \pm 2.4$ kJ/mol (1 cation). This interaction parameter is strictly valid only for Tschermak-substituted $^{[6]}$Al in biotite according to the operational substitution. Application of the suggested garnet-biotite geothermometer reproduces well the reference temperatures of experimental and natural garnet biotite assemblages.

## Introduction

The Fe-Mg exchange between garnet and biotite is strongly temperature dependent and therefore is widely used as a geothermometer. The cation exchange reaction can be expressed as

$$\underset{\text{pyrope}}{Mg_3Al_2Si_3O_{12}} + \underset{\text{annite}}{KFe_3AlSi_3O_{10}(OH)_2} \leftrightarrow \underset{\text{almandine}}{Fe_3Al_2Si_3O_{12}} + \underset{\text{phlogopite}}{KMg_3AlSi_3O_{10}(OH)_2}. \quad (1)$$

Early calibrations of this exchange reaction were based either on natural assemblages for which the *P-T* conditions were constrained by independent methods (e.g., Thompson 1976; Goldman and Albee 1977) or on experimental data (Ferry and Spear 1978; Perchuk and Lavrent'eva 1983 and Perchuk et al. 1985). The two experimental studies differ in starting materials and experimental conditions employed: Ferry and Spear (1978) carried out exchange experiments with synthetic binary (Fe-Mg) phases at temperatures from 550 to 800 °C at 0.2 GPa; Perchuk and Lavrent'eva (1983) used predominantly natural minerals as reactants for their experiments in the temperature range 575 to 1000 °C at 0.55 to 0.6 GPa. All the early calibrations assumed ideal Fe-Mg mixing behavior in both phases. Ideal Fe-Mg mixing in biotite, for example, was suggested by Mueller (1972), Wones (1972), Schulien (1975), and Ganguly (1978) in experimental and empirical investigations, while ideal mixing of Fe and Mg in garnet has been inferred in consideration of a similarity of their ionic radii (Shannon and Prewitt 1969), omitting that thermodynamic ideality is not always simply a function of the sizes of the mixing cations (e.g., Geiger and Rossman 1994).

The application of these calibrations to natural assemblages is restricted, however, because the effects of additional cations, such as Ca and Mn in garnet or Ti, $^{[6]}$Al, and $Fe^{3+}$ in biotite, on the Fe-Mg partitioning between the two phases are not considered (e.g., Saxena 1969, Dallmeyer 1974).

To obtain reliable temperature estimates for a wide compositional range of natural assemblages, a knowledge of the mixing properties of both phases is required. The mixing behavior of quaternary Ca-Mn-Fe-Mg garnets has been extensively studied (e.g., Ganguly and Saxena 1984; Chatterjee 1987; Geiger et al. 1987; Berman 1988, 1990; Hackler and Wood 1989; Koziol and Bohlen 1992; Berman and Aranovich 1996; Ganguly et al. 1996). The at-

* Current address: Bayerisches Geoinstitut, Universität Bayreuth, 95440 Bayreuth, Germany

0003–004X/97/1112–1225$05.00

tempts to determine the mixing properties of biotite focused predominantly on the mixing behavior of Ti and $^{[6]}$Al. These studies are summarized as follows:

(1) Indares and Martignole (1985) derived interaction parameters for $^{[6]}$Ti and $^{[6]}$Al in biotite, on the basis of a combination of the experimental results of Ferry and Spear (1978) and data from granulite facies assemblages, assuming ideal Fe-Mg mixing in biotite and adopting certain garnet activity models (Newton and Haselton 1981; Ganguly and Saxena 1984).

(2) Dasgupta et al. (1991) and Bhattacharya et al. (1992) derived Fe-Mg interaction parameters for biotite by using existing experimental studies and refined garnet activity models.

(3) Patiño Douce and Johnston (1991) and Patiño Douce et al. (1993) undertook melting experiments using natural starting materials and constrained biotite mixing properties for $^{[6]}$Al and $^{[6]}$Ti assuming ideal Fe-Mg mixing, vacancies residing on the M1 site, and ordering behavior between the M1 and M2 sites. The derived Margules parameters ($W_{MgAl}$, $W_{FeAl}$, $W_{AlTi}$-$W_{MgTi}$, $W_{AlTi}$-$W_{FeTi}$) describe the mixing properties of Al, Ti, and $Fe^{3+}$ on the M2 site neglecting cross-site contributions. For the majority of their equilibrated biotites with $X_{Mg} = 0.38 \pm 0.05$, the assumed ordering contradicts the results of Brigatti et al. (1991), who undertook crystal structure refinements on natural biotite and observed ordering only in biotite with $X_{Mg} > 0.5$.

(4) Kleemann and Reinhardt (1994) constrained $W_H$ and $W_S$ Margules parameters for Fe-Mg-Al mixing in biotite on the basis of a comparison of the experimental studies of Ferry and Spear (1978) and Perchuk and Lavrent'eva (1983). The Fe-Mg-Ti biotite mixing parameters and the garnet activity model were taken from Sengupta et al. (1990) and Berman (1990), respectively. They assumed ideal Fe-Mg mixing in biotite and strictly binary biotite for the study of Ferry and Spear (1978), they attributed the difference between this calibration and that of Perchuk and Lavrent'eva (1983) to nonideal mixing behavior of Al in biotite.

(5) Biotite mixing properties obtained from natural metamorphic assemblages were reported, for example, by Williams and Grambling (1990) or Hoisch (1991).

(6) Circone and Navrotsky (1992) performed a calorimetric study on phlogopite-eastonite solid solutions. The results were fitted to both a symmetric and an asymmetric solution model for the Mg-Al mixing in trioctahedral micas.

(7) On the basis of displacement experiments of the breakdown reaction of annite to sandine, magnetite, and $H_2$, Benisek et al. (1996) derived a Margules parameter $W_{AnnSid}$ for simple symmetric Fe-Al mixing in biotite.

The various activity models and respective calibrations of the Fe-Mg exchange equilibrium are restricted to the compositional ranges of the databases employed. In addition, an unequivocal proof of chemical equilibrium is difficult to ascertain, and inferred *P-T* conditions may not be entirely reliable, particularly for the natural assemblages. Moreover, the compositional complexity of natural phases complicates the formulation of mixing models. Experimental studies have, in comparison, certain advantages: The *P-T* conditions are well constrained; the achievement of equilibrium can be ascertained by special techniques; the choice of reactants allows the examination of a simple or complex system; and compositional changes can be correlated with the experimental conditions. Nevertheless, the experimental studies have some drawbacks. Perchuk and Lavrent'eva (1983) and Patino Douce and Johnston (1991) performed experiments using compositional complex natural phases. The former do not report the complete compositions of their equilibrated phases, therefore mixing properties of the additional components cannot be constrained. The experiments of Patino Douce and Johnston (1991) were not reversed. The experimental study of Ferry and Spear (1978) was limited to Fe-rich garnet compositions ($Alm_{90}Py_{10}$, $Alm_{80}Py_{20}$) and tight compositional brackets were only achieved for the $Alm_{90}Py_{10}$ experiments. The range of compositions spanned by their data is therefore too small to determine the Fe-Mg mixing properties of the phases.

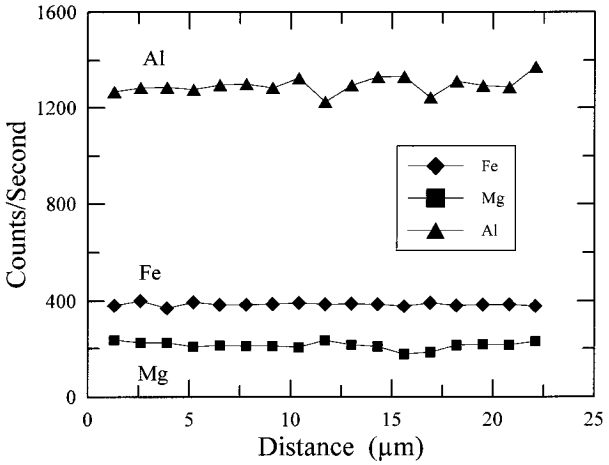


**FIGURE 1.** Element concentration profile across a 24 μm wide garnet crystal ($Alm_{80}Py_{20}$), synthesized at 900 °C and 1.5 GPa.

In view of the difficulties concerning the evaluation of the biotite mixing behavior and the large inconsistencies between existing calibrations of the Fe-Mg exchange (e.g., Kleemann and Reinhardt 1994), further experimental study is needed. In this contribution, we present and discuss new experimental data for the Fe-Mg exchange reaction in the garnet-biotite system to address the following objectives: (1) The exchange mechanisms are examined critically. (2) Possible nonideal Fe-Mg mixing behavior of the phases is investigated. (3) The nonideal mixing in Fe-Mg-Al biotites is evaluated, because the initially binary biotite changed to ternary compositions during the experiments. (4) A garnet-biotite geothermometer involving the derived biotite-mixing properties is estab-

**TABLE 1.** Experimental conditions of Fe-Mg exchange reaction between garnet and biotite

| Experiment (no.) | $T$ (°C) | P (GPa) | Time I.exp./II.exp. (h) | $X_{Fe}^{Bio}$ starting material | $H_2O$ added I.exp./II.exp. (wt%) | Solid redox buffer |
|---|---|---|---|---|---|---|
| 70/11 | 600 | 0.207 | 287 | 0.4 | 12.8 | QFM |
| 70/8 | 600 | 0.207 | 501 | 0.25 | 11.6 | QFM |
| 70/3* | 650 | 0.207 | 99/194 | 0.5 | 11.3/18.4 | QFM |
| 70/4* | 650 | 0.207 | 456/490 | 0.25 | 11.3/15.9 | QFM |
| 70/1* | 700 | 0.207 | 594/144 | 0.5 | 11.5/24.7 | QFM |
| 70/2* | 700 | 0.207 | 597/ 98 | 0.25 | 11.5/22.4 | QFM |
| 70/5* | 750 | 0.207 | 481/240 | 0.5 | 12.9/19.0 | QFM |
| 70/12 | 750 | 0.207 | 235 | 0.4 | 10.3 | QFM |
| 70/9 | 800 | 0.207 | 165 | 0.65 | 13.9 | QFM |
| 70/14 | 800 | 0.207 | 312 | 0.4 | 10.3 | CoCoO |
| 80/12* | 650 | 0.207 | 482/499 | 0.4 | 12.0/ 7.5 | CoCoO |
| 80/1* | 650 | 0.207 | 411/192 | 0.1 | 13.2/18.2 | QFM |
| 80/9 | 700 | 0.207 | 478 | 0.65 | 8.7 | CoCoO |
| 80/6 | 700 | 0.207 | 409 | 0.4 | 13.3 | QFM |
| 80/3* | 750 | 0.207 | 339/212 | 0.65 | 14.5/12.3 | QFM |
| 80/4* | 750 | 0.207 | 430/211 | 0.25 | 10.2/14.1 | QFM |
| 80/11 | 800 | 0.207 | 317 | 0.65 | 8.7 | CoCoO |
| 80/10 | 800 | 0.207 | 311 | 0.4 | 11.0 | CoCoO |

*Note:* Experiment no. 70 = starting garnet composition $Alm_{70}Py_{30}$; no. 80 = $Alm_{80}Py_{20}$; $X_{Fe}^{Bio}$ = Fe/(Fe + Mg); QFM = quartz-fayalite-magnetite buffer, CoCoO = cobalt-cobalt oxide buffer.
* Two-step experiments.

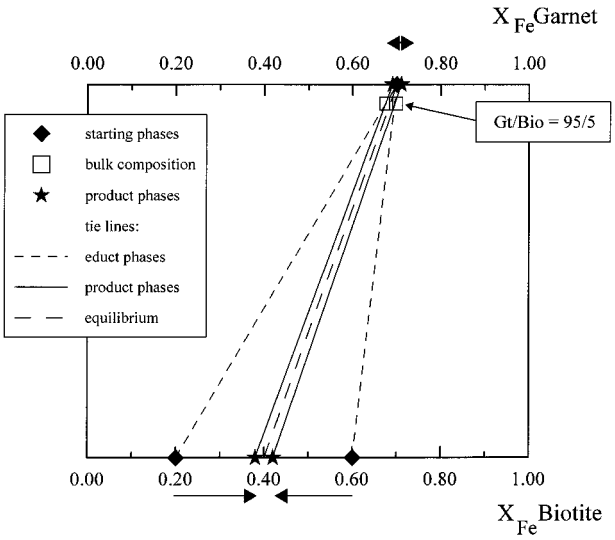


**FIGURE 2.** Schematical sketch showing the experimental design (after Ferry and Spear 1978). The large Gt/Bio ratio (by weight percent) results in only small variations of the garnet composition, whereas the corresponding change of the $X_{Fe}$ in biotite is significant. Arrows along the axes reflect the changes in mineral composition and direction of reaction toward equilibrium. Lines represent tie-lines of corresponding starting phases and product phases, respectively.

lished and applied to experimental and natural garnet-biotite assemblages.

## EXPERIMENTAL TECHNIQUES

### Starting materials

Synthetic phases were used in the cation exchange experiments as reactants. Garnet samples ($Alm_{80}Py_{20}$ and $Alm_{70}Py_{30}$) were synthesized from oxide and silicate mixtures in a piston-cylinder apparatus at 1.5 GPa and 900 °C with experimental duration of 4 h (e.g., Keesmann et al. 1971; Frentrup 1980).

Biotite with the composition $Ann_{50}Phl_{50}$ was provided by Spiering (1972) and biotite samples ($Ann_{10}Phl_{90}$; $Ann_{25}Phl_{75}$; $Ann_{40}Phl_{60}$; $Ann_{65}Phl_{35}$) were synthesized hydrothermally in Tuttle vessels at 740 °C and 0.2 GPa using water as a pressure medium and employing the double capsule buffer technique (Eugster 1957). Oxide mixtures of the required compositions were used as starting materials and held in $Ag_{70}Pd_{30}$ capsules. The oxygen fugacity was controlled by iron-wüstite (IW) solid buffers, which were held in an outer gold capsule (IW, 740 °C: $\log f_{O_2} = -20.0$). The solid buffer was replaced two to three times for each synthesis (e.g., Eugster and Wones 1962; Wones 1963).

The composition and purity of the synthesized minerals were checked by optical examination, X-ray powder diffractometry, and microprobe analysis. The biotite samples were strictly binary and generally close ($X_{Fe} \pm 2$ mol%) to the intended compositions as deduced from mineral stochiometry and X-ray diffractometry. A small deviation between measured and intended composition increases with increasing iron content of biotite (Gessmann 1995).

According to electron microprobe results and XRD data, the garnet compositions were close to those intended ($X_{Alm}$ approximately ± 2 mol%). Line profiles across some synthesized garnet crystals showed compositional zoning with respect to Al, while Fe and Mg distribution were within acceptable limits (Fig. 1). The molar volumes of the garnet are in good agreement to those of Geiger et al. (1987). The $Fe^{3+}$ contents of synthetic almandine generally amount to between 0 and 6% of the total Fe (Woodland and Wood 1989). The contents of $Fe^{3+}$ in the garnet of this study is estimated to be 2% of the total Fe, on the basis of electron microprobe analysis (= total Fe) and wet chemical analysis (= $Fe^{2+}$) following Fritz and Popp (1985).

### Cation-exchange experiments

Synthetic garnet and biotite were ground separately for 20 min and then mixed in a weight ratio of 95% garnet and 5% biotite (Ferry and Spear 1978). The mixture was homogenized by grinding for another 20 min under acetone in an agate mortar.

Starting materials with approximately 10 wt% twice-distilled water were sealed in $Ag_{70}Pd_{30}$ capsules (o.d. 2 mm, i.d. 1.6 mm, length ~20 mm). The silver palladium capsules and solid buffers (QFM, CoCoO) with an appropriate amount of water were sealed in gold capsules (o.d. 3.8 mm, i.d. 3.2 mm, length ~35 mm). The double capsules were placed in horizontally arranged Tuttle vessels using water as the transmitting pressure medium. Temperature was controlled by sheathed NiCr-Ni thermocouples with an accuracy of ± 5 °C. Given the temperature gradient over the length of the capsule (35 to 40

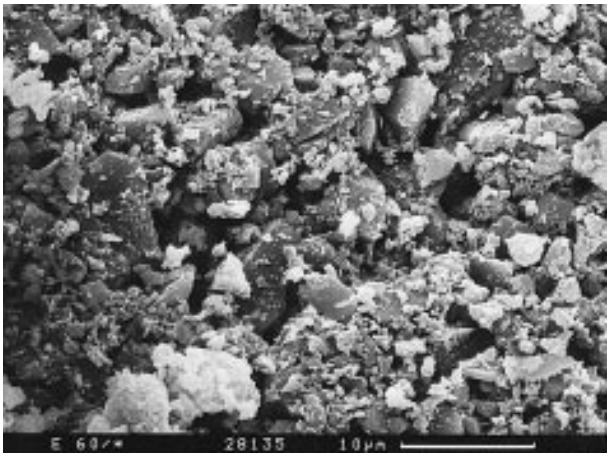


**FIGURE 3.** SEM image of ground starting mixture showing broken and deformed grains of garnet and biotite with a large portion of very small (~1 μm) particles.

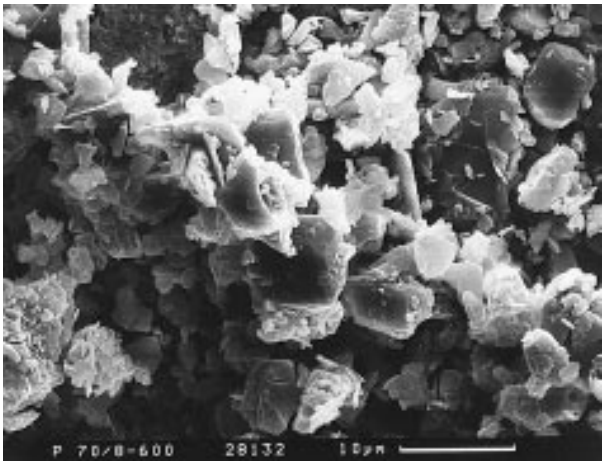


**FIGURE 4.** SEM image of garnet and biotite mixture equilibrated at 600 °C and 0.2 GPa for 20 d showing the development of crystal faces on larger garnet grains and the decreasing amount of smaller particles in comparison with the starting mixture (see Fig. 3).

mm), the total deviation from the nominal temperature is estimated to be ± 10 °C (see also Rudert et al. 1976). Pressure was controlled using a Heise manometer with an accuracy of ±50 bar. The experiments were carried out in the temperature range of 600–800 °C at 0.207 GPa with experimental times varying between 100 and 500 h (Table 1). After the experiments, the presence of the buffer assemblage phases was checked to ascertain that the redox conditions were maintained during the experiment. For a majority of the experiments, additional experiments were required to approach equilibrium more closely. These additional experiments were performed after grinding (30 min) the experimental products of the first experiment following the procedures described above.

The most crucial point of cation exchange experiments is to prove that chemical equilibrium has been achieved. Herein, the bracketing technique was employed by supplying a Fe-rich biotite as well as a Mg-rich biotite as an exchange partner with garnet at a given *P-T* condition. Because of the chosen weight ratio of the phases only minor changes of the garnet composition are required to balance the significant changes in the biotite composition (Fig. 2).

### Preparation and analysis of experimental products

The experimental products were first examined optically to check for the presence of impurities and quench phases, which were not observed.

Electron microprobe analyses of biotite in polished thin sections were generally unsuccessful. The analyses typically reflected garnet-biotite mixtures because of the small modal amount of biotite, its very small grain size (1–10 μm), and its platy habit. The samples were, therefore, prepared for analysis using a suspension method. The experimental products were suspended in 2–5 ml ethanol and dispersed in an ultrasonic bath. A few drops of the suspension were then placed onto a flat surface of artificial resin and were allowed to settle randomly and occasionally as separate grains. The dried suspensions were not polished to avoid damage to the tiny biotite flakes. This method of preparation has the disadvantage that uneven mineral surfaces lead to low chemical analysis totals, especially for the biotite grains. On the other hand, the technique has the advantage that the thin biotite flakes settle in a suitable orientation for electron microprobe analysis and overlapping mineral grains and resulting mixed analyses can be avoided.

The samples were analyzed using a CAMECA electron microprobe (Camebax Microbeam). Operating conditions were 7 nA and 15 kV, the beam size was ~ 1 μm and the counting time was 20 s for the peak and background positions. The analyzed elements were K, Mg, Fe, Al, and Si. Iron metal, MgO, potassium feldspar, and sillimanite were used as standards. Data processing was performed with the PAP correction procedure (Pouchon and Pichoir 1984).

## RESULTS

### Mechanisms of cation exchange

As the attainment and proof of equilibrium is the most important issue of exchange experiments, it is essential to analyze and constrain the effective cation exchange mechanisms. Potential mechanisms of cation exchange in the experimental *P-T-t* ranges are surface reactions (e.g., solution-precipitation) and diffusion. Earlier experimental studies of the Fe-Mg exchange between garnet and biotite (e.g., Ferry and Spear 1978) considered the entire volume of garnet to be involved in the cation exchange with biotite. It is unlikely, however, that this exchange could be achieved solely by diffusion at the experimental conditions given the low diffusion coefficients in garnet (e.g., Chakraborty and Rubie 1996). This raises the question which mechanism dominates the cation exchange and,

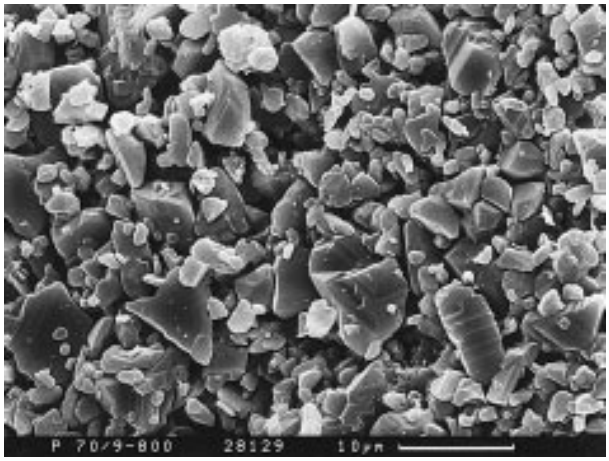


**FIGURE 5.** SEM image of experimental products that were equilibrated at 800 °C and 0.2 GPa for 20 d. The smaller garnet grains exhibit spherical shapes and larger grains show crystal faces.

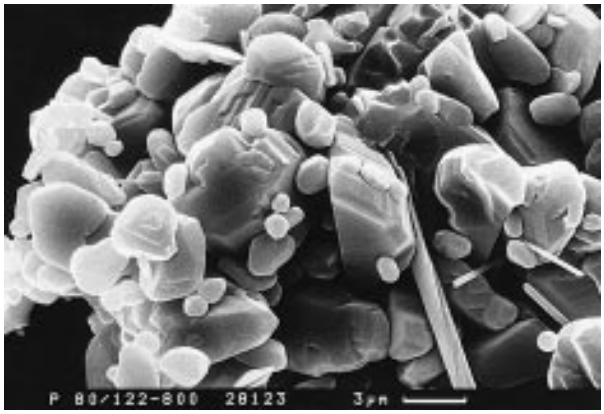


**FIGURE 6.** SEM image showing orthopyroxene crystals developed by a net transfer reaction in an experiment at 800 °C (details see text). The larger garnet grains developed vicinal faces, while the smaller grains attained spherical shapes.

maybe even more importantly, whether or not the entire garnet volume is involved.

**Surface reactions: solution-precipitation**

Diffusion and surface reactions can be distinguished by the characteristics of the compositional zoning: Diffusion creates continuous concentration profiles, whereas solution-precipitation results in discontinuous profiles. Furthermore, surface reactions, in contrast to diffusion, change the size, the shape, or both of the phases involved (e.g., Giletti 1985).

Distinguishing exchange mechanisms by measuring element concentration profiles is not possible in the present study because the profiles are extremely short in garnet and are not detectable by common analytical techniques. However, surface reactions can be identified by a comparison of the grain size distribution and the morphological characteristics of the starting material with the experimental products using scanning electron microscopy (SEM). The two-phase mixture consists of deformed and broken grains with a large proportion of very fine particles ($<1$ μm) (Fig. 3). The final experimental products show evidence of progressive solution and precipitation with increasing temperature (Figs. 4 and 5). The smaller grains decrease in number and attain spherical shapes; whereas the larger grains increase in size and develop crystal and vicinal faces (see also Fig. 6). These observations document the recrystallization of garnet by solution and precipitation, where the larger grains grow at the expense of the smaller grains (Ostwald ripening).

To assess the contribution of the solution-precipitation mechanism to the Fe-Mg exchange, the grain size distributions in a starting and a final mixture (750 °C experiment) were analyzed by laser granulometry. A comparison of the grain size spectra (Fig. 7) confirms the SEM results, that the proportion of particles smaller than 5 μm decreases in the experimental products, while that of larger grains increases.

The volume of dissolved material (predominantly garnet) in the experimental products is estimated from a decrease of the grain size fractions $<5$ μm to be about 48% (Fig. 7). The volume of precipitated material, computed from the grain size fractions $>5$ μm, is too large to compensate the dissolved material. This discrepancy is attributed to the presence of aggregated particles. This interpretation is confirmed by optical observations. The calculated volume of precipitated material is about 50% if grain size fractions $>15$ μm are neglected. Thus, the partitioning of Fe and Mg between garnet and biotite in the experiments is largely controlled by solution and precipitation processes, involving ~50% of the garnet volume at the *P-T-t* conditions of the experiments.

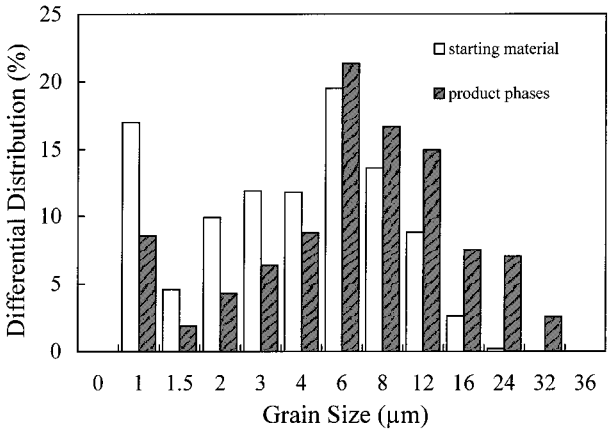


**FIGURE 7.** Histogram showing grain size distribution of starting material and of experimental products equilibrated at 750 °C, 0.2 GPa for 20 d. In the experimental products the smaller grain sizes decrease and the larger grain sizes increase in comparison with the starting material indicating growth of larger grains at the expense of smaller grains.

**TABLE 2.** Compositional data of garnet and biotite and Fe-Mg partition coefficients ($K_D$) of the bracketing experiments

| Experiment (no.) | $T$ (°C) | $X^{Gt}_{Fe}$ | $X^{Gt}_{Mg}$ | $X^{Bio}_{Fe}$ | $X^{Bio}_{Mg}$ | $X^{[6]Al}$ | $K_D$ | $\ln K_D$ | $T_{model} - T_{exp}$ (A) | $T_{model} - T_{exp}$ (B) |
|---|---|---|---|---|---|---|---|---|---|---|
| 70/11 | 600 | 0.690 | 0.310 | 0.324 | 0.606 | 0.070 | 4.163 | 1.426 | −2 | −3 |
| 70/8 | 600 | 0.684 | 0.316 | 0.307 | 0.586 | 0.107 | 4.132 | 1.419 | −35 | −43 |
| 70/3* | 650 | 0.680 | 0.320 | 0.357 | 0.539 | 0.104 | 3.208 | 1.166 | 30 | 35 |
| 70/4* | 650 | 0.685 | 0.315 | 0.349 | 0.546 | 0.105 | 3.402 | 1.224 | 3 | 3 |
| 70/1* | 700 | 0.686 | 0.314 | 0.384 | 0.517 | 0.099 | 2.941 | 1.079 | 34 | 46 |
| 70/2* | 700 | 0.675 | 0.325 | 0.369 | 0.524 | 0.107 | 2.949 | 1.082 | 19 | 28 |
| 70/5* | 750 | 0.697 | 0.303 | 0.437 | 0.419 | 0.144 | 2.206 | 0.791 | † | † |
| 70/12 | 750 | 0.677 | 0.323 | 0.421 | 0.459 | 0.120 | 2.285 | 0.826 | † | † |
| 70/9 | 800 | 0.695 | 0.305 | 0.515 | 0.381 | 0.104 | 1.681 | 0.520 | † | † |
| 70/14 | 800 | 0.691 | 0.309 | 0.520 | 0.355 | 0.125 | 1.527 | 0.423 | † | † |
| 80/1* | 650 | 0.779 | 0.221 | 0.493 | 0.415 | 0.092 | 2.967 | 1.088 | 134 | 144 |
| 80/12* | 650 | 0.783 | 0.217 | 0.435 | 0.482 | 0.083 | 3.998 | 1.386 | −6 | −11 |
| 80/9 | 700 | 0.802 | 0.198 | 0.464 | 0.423 | 0.113 | 3.693 | 1.306 | −39 | −48 |
| 80/6 | 700 | 0.788 | 0.212 | 0.462 | 0.381 | 0.157 | 3.065 | 1.120 | −1 | −10 |
| 80/3* | 750 | 0.809 | 0.191 | 0.499 | 0.382 | 0.119 | 3.242 | 1.176 | −27 | −30 |
| 80/4* | 750 | 0.781 | 0.219 | 0.473 | 0.409 | 0.118 | 3.084 | 1.126 | −15 | −14 |
| 80/11 | 800 | 0.792 | 0.208 | 0.470 | 0.394 | 0.136 | 3.192 | 1.161 | −97 | −103 |
| 80/10 | 800 | 0.770 | 0.230 | 0.491 | 0.398 | 0.112 | 2.714 | 0.998 | −9 | 22 |

*Note:* Pressure = 0.207 GPa; $X_i^{Gt} = il(Fe + Mg)$; $X_i^{Bio} = il(Fe + Mg + {}^{[6]}Al)$; $K_D = (X_{Fe}/X_{Mg})^{Gt}/(X_{Fe}/X_{Mg})^{Bio}$; (**A**), (**B**): Geothermometry employing the respective biotite mixing properties (Table 4) in Equations 11 and 12.

* Two-step experiment.

† Not considered in LSQ regressions.

### Surface reactions: net transfer reaction

The starting compositions of the synthetic biotite were binary annite-phlogopite solid solutions (Table 1). During the experiments their Fe/Mg ratios became more aluminous, with $^{[6]}X_{Al}$ on the order of 0.07 to 0.14 (Table 2), which corresponds to 0.4–0.85 cations per formula unit (22 O atom basis). Figure 8 shows the $^{[6]}$Al contents of the biotite as a function of experimental temperature. Although the scatter of the data is considerable, a temperature dependence can be resolved, as indicated by the regression line. Because the starting biotite compositions were along the annite-phlogopite join, the experiments were not truly bracketed with respect to Al. Nevertheless, the approach to equilibrium compositions is documented for the two-step experiments: The biotite compositions were analyzed after both experiments, showing the direction toward equilibrium. Moreover, the change in Al content was generally smaller in the second experiment (at comparable experimental durations), indicating that the reaction kinetics become progressively slower as equilibrium is approached.

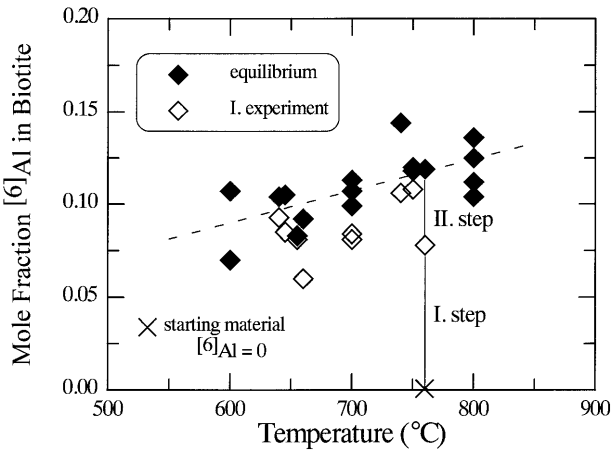


**FIGURE 8.** Octahedral Al contents of equilibrated biotite shown as a function of temperature. The regression line [$^{[6]}X_{Al} = 173 \times 10^{-6} \times T(°C) - 138.44 \times 10^{-4}$] indicates increasing $^{[6]}$Al contents with increasing temperature. The open symbols indicate Al contents in biotite after the first in a two-step experiment, showing the direction toward equilibrium. The starting material consisted of annite-phlogopite$_{ss}$ (i.e., $^{[6]}$Al free).

An evaluation of the biotite stoichiometry indicates that the substitution of Al preferably takes place by the Tschermak substitution (Eq. 2).

$$^{[6]}(Mg, Fe)^{2+} + {}^{[4]}Si^{4+} \leftrightarrow {}^{[6]}Al^{3+} + {}^{[4]}Al^{3+} \quad (2)$$

Figure 9 shows the compositions of the equilibrated biotites. The Tschermak and muscovite substitutions are indicated by lines. The line denoting the Tschermak reaction also indicates completely filled octahedral sites. The biotite compositions of this study fall close to this line, implying that substitution of Al is dominated by the Tschermak substitution and that vacancies are negligible. However, the equilibrated biotite samples have significant deficiencies (up to 40%) in their K contents, which is explained by the talc substitution (Eq. 3). Because no potassium minerals were detected in the experimental charges, K is believed to remain in the fluid.

$$^{[12]}K^{+} + {}^{[4]}Al^{3+} \leftrightarrow {}^{[12]}\square + {}^{[4]}Si^{4+} \quad (3)$$

The tetrahedral substitutions in Reactions 2 and 3 proceed in opposite directions. Hence the amount of octahedral Al [$^{[6]}Al = (Si_{tot} + Al_{tot}) - 8$] in most of the biotite is not balanced by the amount of excess $^{[4]}$Al ($^{[4]}Al_{exc} = 6 - Si_{tot}$) although the $^{[6]}$Al is essentially substituted by the Tschermak reaction. Increasing Si content and an increasing amount of $^{[6]}$Al that is not balanced by $^{[4]}Al_{exc}$, as a function of decreasing K content in biotite, both give evidence for the talc substitution.

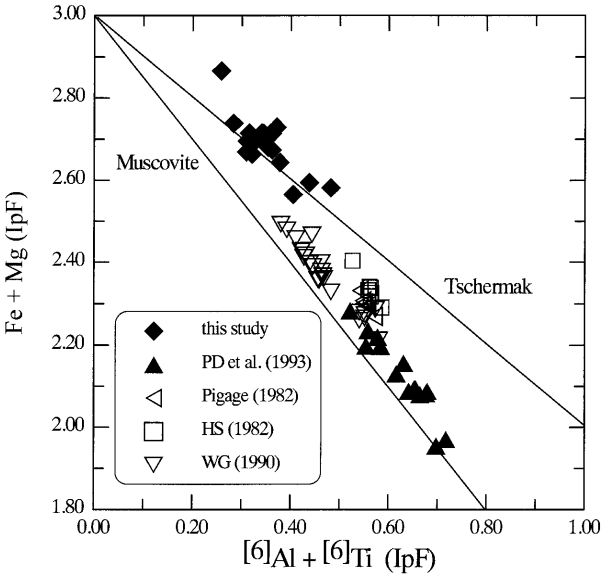


**FIGURE 9.** Compositions of experimental and natural biotite on octahedral sites. The lines denote Al substitution. The Tschermak substitution line also indicates completely filled octahedral sites. Compositions falling below this line imply the presence of octahedral vacancies. Besides this study all other biotites shown, contain both Ti and Al. (IpF = Ions per formula unit; PD et al. = Patino Douce et al. 1993; HS = Hodges and Spear 1982; WG = Williams and Grambling 1990).

The incorporation of Al in pyroxenes equilibrated with garnet has been observed in other Fe-Mg exchange experiments (e.g., Pattison and Newton 1989; Eckert and Bohlen 1992). Pattison (1994) argued that the incorporation of Al into Fe-Mg phases during exchange experiments takes place by surface reaction (e.g., multicomponent solution and precipitation) rather than diffusion.

The large garnet-biotite ratio (95/5) here provides a bulk alumina content > 21 wt%, and the most probable source of Al in our study is garnet. If the incorporation of Al into biotite took place by a reaction, i.e., the breakdown of garnet, it must have been accompanied by formation of other phases, e.g., orthopyroxene. Evidence for such a net transfer reaction was found in experiments at temperatures above 750 °C, where euhedral needles of orthopyroxene were observed by SEM (Fig. 6). The absence of orthopyroxene in experimental products at lower temperature (< 750 °C) may be due to sluggish rates or to *P-T* conditions not suitable for the growth of orthopyroxene. A model reaction, which could account for the formation of orthopyroxene as well as for the change of biotite solid solutions toward Al-rich compositions, is:

$$\underset{\text{garnet}_{ss}}{(Mg, Fe)_3Al_2Si_3O_{12}} + \underset{\text{annite-phlogopite}_{ss}}{2K_2(Fe, Mg)_6Al_2Si_6O_{20}(OH)_4}$$

$$\leftrightarrow \underset{\text{orthopyroxenes}}{2(Fe, Mg)_2Si_2O_6} + \underset{\text{eastonite-siderophyllite}_{ss}}{2K_2(Fe, Mg)_{5.5}Al_3Si_{5.5}O_{20}(OH)_4} \quad (4)$$

Because of the volumetric predominance of garnet, the small modal amount of orthopyroxene formed in such a reaction cannot be detected by X-ray powder diffractometry. Orthopyroxene crystals in the higher-temperature experiments were analyzed with difficulty by use of the electron microprobe. Despite the rare analyses, equilibrium is indicated by Gt-Opx thermometry (Lee and Ganguly 1988) for a few experiments (80/3, 750 °C; 80/10, 800 °C; 80/11, 800 °C) yielding temperatures deviating +74, +15, and −39 °C, respectively, from the experimental temperatures. Moreover the formation of a new phase by a net transfer reaction takes place at, or very close to, chemical equilibrium with the other phases (e.g., Giletti 1985). As a consequence, the presence of a third Fe-Mg phase in the experimental products and its possible influence on the Fe-Mg partitioning between garnet and biotite is considered to be negligible.

### Diffusion in garnet

Although Fe-Mg diffusion in biotite can be expected to be sufficiently fast at the chosen experimental conditions to reach equilibrium compositions (e.g., Dowty 1980; Pattison 1994), recent studies on Fe-Mg diffusion in garnet (e.g., Cygan and Lasaga 1985; Chakraborty and Ganguly 1991, 1992; Chakraborty and Rubie 1996) have shown very low diffusion coefficients, thus indicating that Fe and Mg diffusion profiles in garnet are extremely short (<1 μm), and thus complete Fe-Mg exchange in garnet may not be achieved by diffusion in the duration of the experiments. Although the preceding evaluation gave unequivocal evidence for solution-precipitation as the dominant exchange mechanism, a finite amount of diffusion (at least at higher temperatures) may contribute to the cation exchange.

Aiming to obtain a rough estimate for the upper limit by which diffusion possibly supplements the surface reactions, a simple model calculation was performed with the following simplifications. (1) The changing grain sizes, resulting from surface reactions, were neglected. (2) Tracer diffusion coefficients instead of chemical diffusion coefficients were employed. (3) Discontinuous diffusion profiles and a mean grain size of 5 μm were assumed. On the basis of the diffusion equation of Crank (1975) and the diffusion data of Chakraborty and Rubie (1996), who performed Mg tracer diffusion experiments in garnet under $T$-$f_{O_2}$ conditions comparable to those presented here, it is estimated that up to 20 vol% of garnet could react by diffusion at 800 °C and 20 d.

### Mass balance constraints

From the observed Fe/Mg changes in biotite composition and the known proportions of the phases, the corresponding changes in garnet composition, which would result from equilibration with biotite, can be calculated. Such mass balance calculations were performed for variable volumes of garnet participating in the Fe-Mg exchange. Table 3 gives the results of such mass balance calculations for two experiments. Case A was computed

**TABLE 3.** Compositional changes of garnet (Δ almandine) according to mass balance calculations for two cases (A) and (B), and assumed volume fractions of garnet participating in the cation exchange

| Garnet involved in cation exchange (vol%) | (A) $\Delta_{Ann}$ = 7.8 mol% Δ almandine (mol%) | (B) $\Delta_{Ann}$ = 19.5 mol% Δ almandine (mol%) |
|---|---|---|
| 100 | 0.41 | 1.03 |
| 95 | 0.43 | 1.08 |
| 90 | 0.46 | 1.14 |
| 80 | 0.51 | 1.28 |
| 70 | 0.59 | 1.46 |
| 60 | 0.68 | 1.71 |
| 50 | 0.82 | 2.05 |
| 40 | 1.03 | 2.56 |
| *30* | 1.37 | *3.42* |
| 20 | 2.05 | 5.13 |
| *10* | *4.11* | 10.3 |
| 5 | 8.21 | 20.5 |

*Note:* Calculations in case (A) are based on an experiment with a change in biotite composition that is representative for most of the experiments, whereas case (B) is based on an experiment with a very large compositional change of biotite. Hence the computed variations in garnet composition for case (B) represent maximum values. Calculations assume a mean grain size of 5 μm. Italics represents vol% garnet and corresponding calculated change in garnet composition, which exceed the 1σ deviation of the microprobe-analysis (~ ±2 mol%).

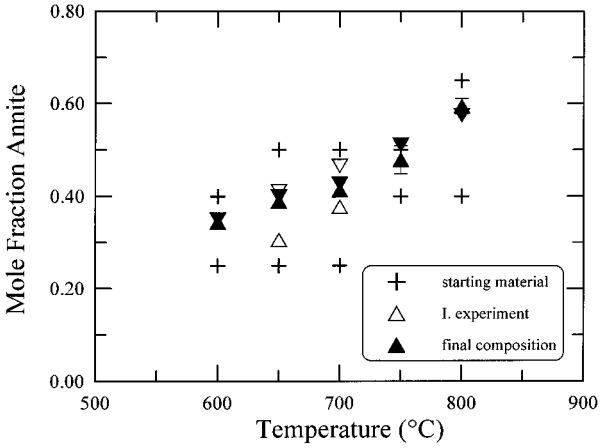


**FIGURE 10.** Annite content of biotite before and after the experiments [$X_{Ann}$ = Fe/(Fe + Mg)] vs. temperature shown for a series of experiments with garnet $Alm_{70}Py_{30}$. Open symbols reflect incomplete cation exchange after a first experiment. The two-step technique assures a close approach to equilibrium compositions (filled symbols). For clarity the 1σ standard deviation is given as an example only for a few experiments.

for a moderate change in biotite composition ($\Delta_{Ann}$ = 7.8 mol%), which is representative for most of the experiments, and case B for an extreme shift in biotite composition ($\Delta_{Ann}$ = 19.5 mol%). The mass balance calculations show that, except for very small exchange volumes (10 and 30 vol% for the two cases, respectively), the almandine content of garnet varies from 0.4 to 2.5 mol%, which is within the uncertainty of the microprobe analysis (approximately ± 2 mol% Alm). Considering the SEM and laser-granulometry results, the volume proportion of garnet participating by surface reactions in the Fe-Mg exchange alone (omitting diffusional contributions and extended reaction times of two-step experiments) would exceed the critical values given in Table 3. Moreover, the mass balance computations prove the effectiveness of the experimental design: The large Gt/Bio ratio assures that the garnet composition remains essentially constant. However, this conclusion will not hold for distinctly lower Gt/Bio ratios.

### Attainment of equilibrium

''Equilibrium'' compositions obtained in exchange experiments might be equivocal if multicomponent solution and precipitation is the operating mechanism (Pattison 1994). The general criteria for the demonstration of chemical equilibrium, such as reversibility or the determination of the direction toward equilibrium composition, cannot be proved in such experiments. Although solution-precipitation was shown to be the dominant exchange mechanism, the achievement of chemical brackets is indicated by the following observations. First, the direction of reaction is demonstrated for all two-step experiments. Because biotite was analyzed after the first and second experiment, there are two biotite compositions marking the direction of reaction between the starting and the final composition as illustrated in Figure 10. The narrow brackets demonstrate the effectiveness of the two-step technique to approach equilibrium. Second, the change in biotite composition during the second experiment, for comparable experimental times, was generally smaller than in the preceding experiment, in agreement with a slowing of the reaction kinetics as equilibrium is approached (Fig. 10). Third, close correspondence of biotite compositions of single experiments and two-step experiments indicates the attainment of equilibrium for both (Fig. 10). Fourth, the partitioning behavior reproduces well with slight variations in experimental conditions, e.g., starting material (Gessmann 1995).

## EVALUATION OF THERMODYNAMIC DATA

### Partition coefficients

For all experiments, both mineral phases were analyzed by electron microprobe. As a result of the preparation technique, only rim compositions of garnet were measured. The changes in garnet composition are generally within the standard deviation of the starting composition. The activity of a component $i$ in garnet and biotite can be written $a_i = (X_i\gamma_i)^3$, where $X$ is the mol fraction and γ the activity coefficient of component $i$. Accordingly, the equilibrium constant is $K_{eq}^{1/3} = K_D K_\gamma$, where the partition coefficient is defined as $K_D = (X_{Fe}/X_{Mg})^{Gt}/(X_{Fe}/X_{Mg})^{Bio}$. It was calculated from an average of 5 to 20 analyses for both minerals.

The partition coefficients are listed in Table 2 and are plotted as a function of inverse temperature in Figure 11. The calibration of Ferry and Spear (1978), which is based

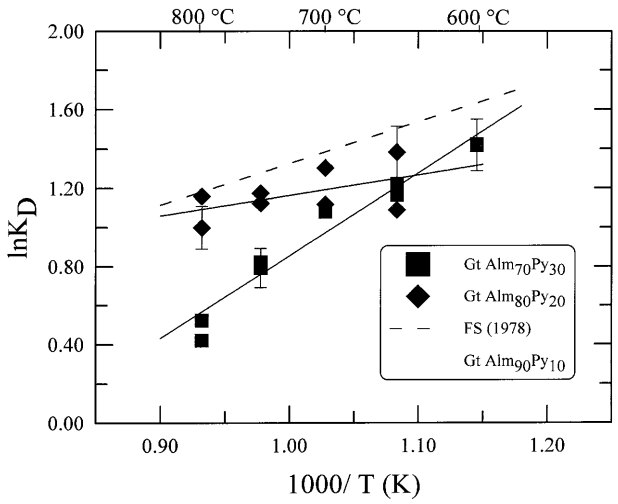


**FIGURE 11.** Partition coefficients [$K_D = (X_{Fe}/X_{Mg})^{Gt}/(X_{Fe}/X_{Mg})^{Bio}$)] for two experiment series and for the calibration of Ferry and Spear (1978) (FS) as a function of inverse temperature. Very tight brackets for the 600 and 700 °C experiments with $Alm_{70}Py_{30}$ result in overlap of the symbols.

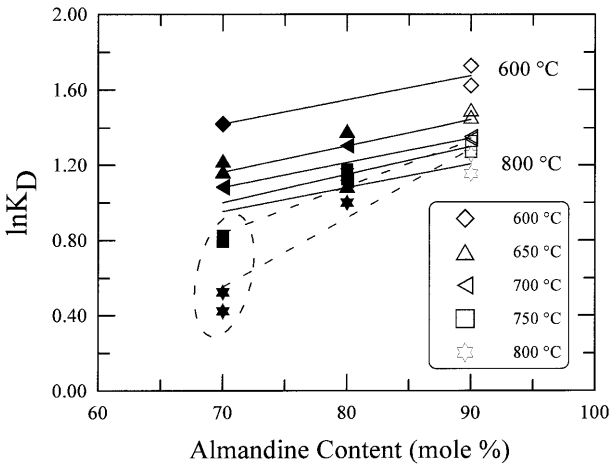


**FIGURE 12.** Fe-Mg partition coefficients as a function of garnet composition [filled symbols = this study; open symbols = Ferry and Spear (1978)]. Regression lines reflect the different experimental temperatures. Disregard of the circled high temperature data allows extrapolation to the almandine end-member.

on exchange experiments with garnet $Alm_{90}Py_{10}$ is shown for comparison. Uncertainties are shown for only a few representative experiments. The total error consists of the uncertainties in temperature and pressure (±10 °C and ± 50 bars, respectively), and the 1σ standard deviations from the microprobe analysis. Error propagation leads to an uncertainty in the partition coefficients on the order of 10–5%, which represent maximum errors because the interdependence of the variables is not considered (e.g., Hodges and McKenna 1987; Dachs 1994).

The partition coefficients do not show a single linear relation with respect to inverse temperature (Fig. 11), which indicates nonideal mixing behavior of either one or both of the phases. Progressively lower $K_D$ values are obtained with increasing Mg content in garnet. The steep regression line for results with garnet $Alm_{70}Py_{30}$ requires attention. It appears that a steeper slope is required to fit the high-temperature data. The presentation of the partition coefficients vs. the Fe content of garnet (Fig. 12) also emphasizes the nonideal mixing behavior and a deviation of the $Alm_{70}Py_{30}$ high-temperature partitioning data. Figures 11 and 12 indicate that the high-temperature data of this experiment series may contain some inconsistencies.

This observation could be due to disequilibrium or to instability of the phases at the experimental pressures and temperatures. Careful examination of the samples by optical microscopy and electron microprobe analysis, however, gave no indication for disequilibrium features. The tight brackets for these experiments suggest that equilibrium was achieved, although the biotite samples of the 800 °C experiments show compositional overlap, which is sometimes observed in experimental studies (e.g., Perkins et al. 1981), but may be attributed to surface reaction and taken as an argument against the achievement of chemical brackets (Pattison 1994). The divergent $Alm_{70}Py_{30}$ high-temperature experiments may also be due to an increased solubility or to instability of biotite at the experimental conditions. Experiments with more Mg-rich garnets ($Alm_{60}Py_{40}$) were not successful. The minor amount or the absence of biotite in the experimental products suggests that for Mg-rich bulk compositions at the given *P-T* conditions biotite is not stable in the presence of garnet. Experiments with Ti- and F-bearing biotite (Gessmann et al. 1994; Gessmann 1995) support the instability argument: both Ti and F increase the thermal stability of Mg-rich biotite (e.g., Forbes and Flower 1974; Munoz 1984; Peterson et al. 1991), and the partition coefficients in the Ti-bearing garnet-biotite system do not show comparable inconsistencies for Mg-rich bulk compositions. Therefore, we conclude that an instability of biotite or an increased biotite solubility at experimental conditions is responsible for the deviation of the $Alm_{30}Py_{70}$ experiments. Disregarding these high-temperature data flattens the slope of the linear regression for the Mg-rich set of experiments. The data can also be fitted to linear equations parallel to the calibration of Ferry and Spear (1978). However, the observed systematic deviation of the partition coefficients from one single linear equation with increasing Mg content of garnet remains true (Fig. 13).

### Application of garnet activity models

In a first attempt to constrain the observed nonideal effects on the Fe-Mg distribution, the mixing properties of garnet are considered. If the effect of nonideality on the partitioning data can be attributed solely to nonideal mixing behavior in garnet, the correction with an appropriate garnet mixing model should result in convergence of the partitioning data. The application of various activ-

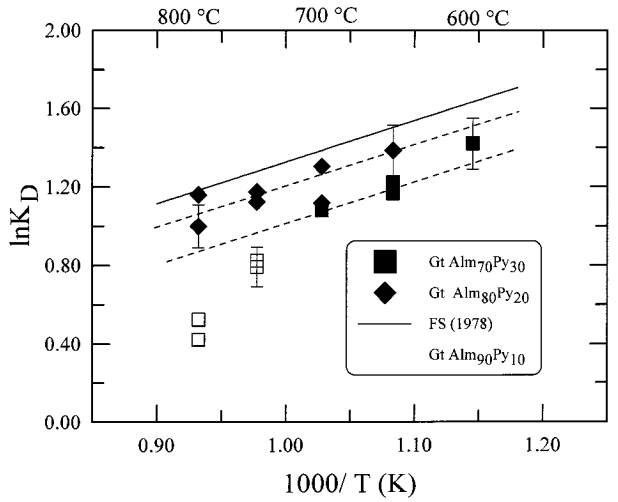


**FIGURE 13.** Fe-Mg partition coefficients between garnet and biotite as a function of inverse temperature. Disregard of the high-temperature data of the Mg-rich experiments (open symbols) allows the calibration line of Ferry and Spear (1978) to be shifted parallel to fit the experimental results of this study.

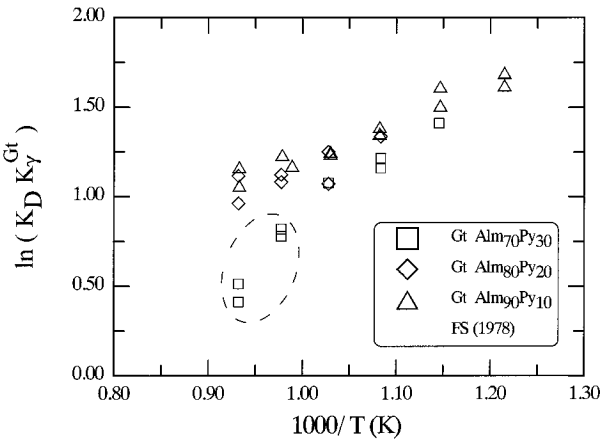


**FIGURE 14.** Diagram showing the Fe-Mg partition coefficients $\ln(K_D K_\gamma^{Gt})$ obtained by application of the garnet mixing model of Berman (1990) to the partitioning data given in Table 2 and to those given by Ferry and Spear (1978) (FS) as a function of inverse temperature. The circled data correspond to the high-temperature experiments with garnet $Alm_{70}Py_{30}$ (see also Figs. 12 and 13 and text).

ity models for Fe-Mg garnets (Ganguly and Saxena 1984; Geiger et al. 1987; Hackler and Wood 1989; Berman 1990; Berman and Aranovich 1996), however, does not lead to a close convergence of the data. The application of asymmetric, highly nonideal Fe-Mg mixing models (Ganguly and Saxena 1984; Geiger et al. 1987), lead to an even wider spread of the data. The garnet activity models of Hackler and Wood (1989), Berman (1990), and Berman and Aranovich (1996) slightly reduce the scatter of the partitioning data, but still do not completely describe the observed nonidealities. As an example, Figure 14 shows the $\ln(K_D K_\gamma^{Gt})$ data using the garnet activity model of Berman (1990). Again, the data for the high-temperature experiments with $Alm_{70}Py_{30}$ garnet deviate significantly from the other results. Disregarding these data yields reasonably converged partition coefficients, suggesting that the Berman garnet model for Fe-Mg garnet solid solutions yields an appropriate fit to the experimental data. This analysis suggests that nonideal mixing effects in biotite must contribute to the observed nonidealities, because none of the applied garnet mixing models could entirely compensate for the observed nonideal effects.

### End-member extrapolation

The ln$K$ values form a curved surface in the $P$-$1/T$ space (if $Cp$ is not negligible), but it may be described by an approximately linear relation at constant pressure in a limited temperature range. The $\ln K_D$ systematics herein appear almost linear suggesting an extrapolation to an end-member. At equilibrium the standard change of free energy is $\Delta\mu^0 = -RT\ln K$ and an extrapolation of experimentally obtained partition coefficients (with $RT\ln K = 3RT\ln K_D + 3RT\ln K_\gamma^{Grt} - 3RT\ln K_\gamma^{Bio}$) to an end-member and comparison with thermodynamic properties for the end-member reaction (where $RT\ln K\gamma = 0$) may provide some information about the mixing properties of the phases. It is assumed that the extrapolation to an garnet end-member cancels garnet nonidealities while those of biotite remain and vice versa.

The data of the present study were combined with the $Alm_{90}Py_{10}$-data of Ferry and Spear (1978), regressed and extrapolated to almandine garnet for each experimental temperature (see Fig. 12). The corresponding $\ln K_{extr}$ are compared to ln$K$ values calculated for the respective $T$ range and 2 kbar from Berman (1988, 1990) (Fig. 15). The difference probably does not reflect only uncertainties in the partitioning data or those due to the graphical approach. The difference instead may be attributed to nonideal mixing in biotite.

An alternative approach, the extrapolation of the experimental partitioning data to a pure Fe-biotite requires the assessment of Al contents in the equilibrated biotite reported by Ferry and Spear (1978). They did not analyze their equilibrated biotite samples for Al but the incorporation of Al into biotite samples of their experiments has to be expected in view of the results presented here and the similarity of experimental design. To assess the Al contents in their biotite, the temperature dependence of $^{[6]}$Al contents (Fig. 8) was extrapolated to the $Alm_{90}Py_{10}$ data. This procedure does not change the Fe/Mg ratio, nor the partition coefficients, but is associated with a relatively large uncertainty because of the low Al contents of biotite. The partition coefficients were corrected for nonideal mixing in garnet (Berman 1990) and then extrapolated to annite. This procedure should cancel nonideal contributions of both garnet and biotite. The extrapolation to annite reveals standard energies $\Delta H_R^0 = -50905$ J/mol (slope) and $\Delta S_R^0 = -17.18$ J/(mol·K) (intercept) in

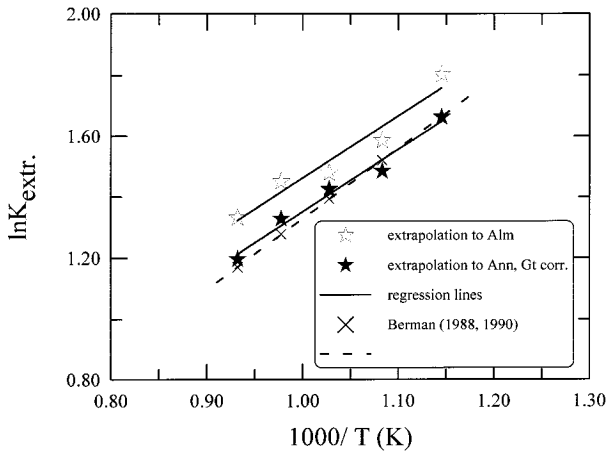


**FIGURE 15.** $\ln K_{extr}$ values vs. inverse temperature as obtained by extrapolation of the $K_D$ data to almandine and to annite (for details see text). The resulting standard energies of reaction are $\Delta H^0_R = -50905$ J/mol and $\Delta S^0_R = -17.18$ J/(mol·K) (extrapolation to annite, after employing the garnet activity model of Berman 1990). The respecitve ln$K$ values calculated with the thermodynamic data of Berman (1988, 1990) are shown for comparison (yielding $\Delta H^0_R = -57594$ J/mol and $\Delta S^0_R = -24.44$ J/(mol·K) for the shown $T$ range at 0.2 GPa).

reasonable accordance with those calculated from the Berman (1988, 1990) data set (Fig. 15).

Berman (1990) derived the standard energies of formation for annite on the basis of experiments of Ferry and Spear (1978), assuming strictly binary compositions and ideal Fe-Mg mixing in biotite. This is equivocal according to the present results. Consequently, the thermodynamic data for annite in the data set of Berman (1988, 1990) are probably valid for an Al-bearing composition and may need reconsideration. On the other hand, the good agreement between the extrapolation and the Berman data suggests only small uncertainties in the annite properties. However, a quantification of the annite properties on the basis of the presented results was not attempted in view of large uncertainties of the graphical approach.

### Least squares computations

Biotite interaction parameters were fitted utilizing a least squares fit (LSQ) program (Deming 1943). The thermodynamic equation that describes Reaction 1 can be formulated as follows:

$$0 = \Delta H^0_R + \int_{298}^{T} \Delta C_P \mathrm{d}T + \int_{1}^{P} \Delta V^0_R \mathrm{d}P - T\left(\Delta S^0_R + \int_{298}^{T} (\Delta C_P/T)\mathrm{d}T\right) + 3\mathrm{R}T \ln K_D + \Delta G_{excess} \quad (5)$$

where

$$\Delta G_{excess} = 3\mathrm{R}T \ln K\gamma^{Gt} - 3\mathrm{R}T \ln K\gamma^{Bio}$$

with

$$K\gamma^{Gt} = (\gamma_{Fe}/\gamma_{Mg})^{Gt} \quad \text{and} \quad K\gamma^{Bio} = (\gamma_{Fe}/\gamma_{Mg})^{Bio}$$

$\Delta H^0_R$, $\Delta S^0_R$, $\Delta V^0_R$, and $\Delta C_P$ are the standard thermodynamic properties, R is the gas constant and $\gamma_i$ is the activity coefficient of component $i$ in the solid solution, $P$ and $T$ are pressure and temperature, respectively. The $\Delta G_{excess}$ term accounts for nonideal mixing behavior of the two phases and has to be described by appropriate activity models, for example, an asymmetric mixing model for Fe and Mg in garnet (e.g., Berman 1990) where,

$$3\mathrm{R}T \ln K\gamma^{Gt} = 3\mathrm{R}T \ln K(\gamma_{Fe}/\gamma_{Mg})^{Gt} = W_{MgFe}(X^2_{Mg} - 2X_{Mg}X_{Fe}) + W_{FeMg}(2X_{Mg}X_{Fe} - X^2_{Fe}) \quad (6)$$

with

$$X_i = i/(\mathrm{Mg} + \mathrm{Fe})$$

or symmetric mixing of Fe and Mg in biotite, (neglecting Al):

$$3\mathrm{R}T \ln K\gamma^{Bio} = 3\mathrm{R}T \ln K(\gamma_{Fe}/\gamma_{Mg})^{Bio} = W_{FeMg}(X_{Mg} - X_{Fe}) \quad (7)$$

with

$$X_i = i/(\mathrm{Fe} + \mathrm{Mg})$$

or symmetric mixing behavior, for the three component Fe-Mg-Al system (e.g., Indares and Martignole 1985):

$$3\mathrm{R}T \ln K\gamma^{Bio} = 3\mathrm{R}T \ln K(\gamma_{Fe}/\gamma_{Mg})^{Bio} = W_{FeMg}(X_{Mg} - X_{Fe}) + (W_{FeAl} - W_{MgAl})X_{Al} \quad (8)$$

with

$$X_i = i/(\mathrm{Fe} + \mathrm{Mg} + {}^{[6]}\mathrm{Al}).$$

Insertion of appropriate garnet and biotite activity models (e.g., Eqs. 6–8) into Equation 5 leads to the final expression for the computer modeling. The standard state properties, the biotite and garnet compositions, the partition coefficients $K_D$, and the $P$-$T$ conditions of the cation exchange experiments were used as input data. Only the experimental results of this study (Table 2, except the high-temperature experiments with garnet $Alm_{70}Py_{30}$) provided the database for the LSQ computations. The interaction parameters for garnet were also used as input data, because the Fe-Mg exchange between the phases is interdependent and their excess mixing terms should not be evaluated simultaneously (e.g., Hackler and Wood 1989).

Fitting the experimental data to the Equation 5 requires the following assumptions: First, chemical equilibrium was achieved. Second, the adopted thermodynamic standard energies of the reaction are correct. Although our results indicate that some nonideal contributions because of Al in biotite might be buried in the thermodynamic

data of Berman (1988, 1990), we apply these values for the least square computations, because Berman's thermodynamic database is widely accepted and commonly used. LSQ computations with other standard energies, e.g., those obtained by extrapolation, are given for comparison. Third, the employed activity model describes the Fe-Mg mixing properties of garnet accurately. Fourth, the adopted mixing model for biotite is correct. We did not model the experimental data assuming an activity model, as suggested by Patino Douce and Johnston (1993) because most of the equilibrated biotites have $X_{Mg}$ values below or close to 0.5 and should not exhibit any ordering corresponding to Brigatti et al. (1991). An asymmetric activity model for a three-component system includes too many unknowns to be fitted accurately with the current database. Attempts to neglect Al in biotite and model Fe-Mg mixing in biotite by using an asymmetric activity model does not yield reasonable values. Very large $W$ terms with large uncertainties were obtained by fitting the distribution coefficients to temperature-dependent activity models for biotite as suggested by Kleemann and Reinhardt (1994). Therefore, the modeling was performed with simple symmetrical mixing models as for example given in Equation 8. Fifth, complications arising from $Fe^{3+}$ and vacancies in both phases are considered. The amount of $Fe^{3+}$ in garnet and vacancies in biotite were shown to be low and are therefore neglected. Neglecting the $Fe^{3+}$ contents in biotite may result in incorrect $K_D$ values and consequently erroneous mixing properties (e.g., Wones and Eugster 1965; Mueller 1972). Moreover the four component system is treated as a ternary system, and nonideal mixing properties of $Fe^{3+}$ will be absorbed in the other interaction parameters (e.g., Ganguly and Saxena 1987). It is not possible to measure the $Fe^{3+}$ contents of the biotite samples by Mössbauer spectroscopy, because of the small modal amount (5%) and its small grain size. A recent investigation of Redhammer et al. (1995) provides Mössbauer data for synthetic annite-phlogopite$_{ss}$. They report $Fe^{3+}$ contents between 1 and 20% of the total Fe. On the basis of their results for the biotite solid solution $Ann_{40}Phl_{60}$ (which is within ± 10 mol% annite content for most of the compositions in this study), the $Fe^{3+}$ contents of the biotites in this study were estimated. The estimated $Fe^{3+}$ contents in biotite reach up to 15% of the total Fe and the absolute values range between $^{[6]}X_{Fe^{3+}} = 0.025$ and 0.07, which are much smaller than the $^{[6]}$Al contents. These estimates are likely to be maximum values because the results of Redhammer et al. (1995) were obtained for biotite with very low $^{[6]}$Al contents and because they do not account for the compositional dependence, i.e., increasing $Fe^{3+}$ content with increasing total Fe content. Therefore, $Fe^{3+}$ in the present biotite is estimated to be low, and the influence of $Fe^{3+}$ was neglected.

## Biotite mixing properties assuming $Fe_{tot} = Fe^{2+}$

### Fe-Mg mixing

LSQ computations employing the garnet activity model of Berman (1990) and the symmetric mixing model for biotite (Eq. 7) have been performed including the data of Ferry and Spear (1978) (12 experiments with garnet $Alm_{90}Py_{10}$). This results in $W_{FeMg} = -7845 \pm 5950$ J/mol, $W_{FeMg} = -9847 \pm 4300$ J/mol, and $W_{FeMg} = -4334 \pm 4650$ J/mol for the three sets of end-member thermodynamic properties (see footnote, Table 4), respectively. The errors are large, nearly exceeding the relatively small, negative values (3 cations), indicating, that the Fe-Mg mixing in biotite is probably close to ideal and that the observed nonidealities should be attributed to Al interactions.

### Fe-Mg-Al mixing

The biotite interaction parameters obtained by least-squares analysis considering ternary interactions in biotite (Eq. 8) and various garnet mixing models are listed in Table 4. Because the different garnet activity models contrast markedly, the differences between the fitted Margules parameters obtained for biotite are expected. However, the $W_{FeMg}$ values are relatively small, whereas the computed numbers for the difference between $W_{FeAl}$ and $W_{MgAl}$ (hereafter referred to as $\Delta W_{Al}$) are comparably large, irrespective of the garnet activity model. The preferred results, adopting the Berman (1990) garnet activity model are given in italics (Table 4). Employing the standard state properties extracted by extrapolation yields interaction parameters that are very similar to the preferred result, while computations including the data of Berman and Aranovich (1996) results in a distinctly lower $\Delta W_{Al}$. The LSQ computations indicate very small Fe-Mg interactions, while significant nonideal mixing between Fe, Mg, and Al in biotite is constrained by large $\Delta W_{Al}$ terms.

## Discussion

A comparison of the $\Delta W_{Al}$ interaction parameter derived herein that is valid for Al-Tschermak substituted Al (Fig. 9) to $W$ terms obtained from vacancy, $^{[6]}Al_{exc}$, or $^{[4]}Al_{exc}$ bearing biotite samples may be inadequate because the latter cannot be attributed solely to the Tschermak substitution (for discussion see Benisek et al. 1996). Instead, a comparison may be possible with interaction parameters that were derived for preferentially Tschermak substituted biotite samples. This criterion is met by the investigations of Circone and Navrotsky (1992) and Benisek et al. (1996), which provide mixing properties for Mg-Al and Fe-Al mixing in trioctahedral micas, respectively. The interaction parameters are $W_{AnnSid} = -29 \pm 4$ kJ/mol derived from displacement experiments (Benisek et al. 1996) and $W_{H,MgAl} = 22.8 \pm 18.7$ kJ/mol derived from calorimetric data (Circone and Navrotsky 1992). Although the latter authors prefer an asymmetric mixing model for the investigated binary, both solution models allow a sufficient fit to their data and, we use their symmetric solution model for comparison. The combination of these results yields $W_{AnnSid} - W_{H,MgAl} = -51.8 \pm 16$ kJ/mol. This value is very close to the $\Delta W_{Al} = -52.7 \pm 7.1$ kJ/mol obtained in this study (italics in Table 4), al-

**TABLE 4.** Summary of the biotite interaction parameters for symmetric mixing in biotite (three cations), calculated by using various garnet activity models

| Garnet mixing model | Standard state properties | Biotite $W_{FeMg}$ | Biotite $W_{FeAl} - W_{MgAl}$ | |
|---|---|---|---|---|
| Berman (1990) | (1) | −6793 | −52 657 | |
| | | ±4700 | ±7 150 | |
| HW (1989) | (1) | 665 | −96 557 | |
| | | ±5200 | ±7 750 | |
| GS (1984) | (1) | 10 540 | −110 197 | |
| | | ±5570 | ±8 300 | |
| Geiger et al. (1987) | (1) | 19 780 | −71 439 | |
| | | ±4550 | ±7 150 | |
| BA (1996) | (2) | −8652 | −35 552 | |
| | | ±4700 | ±7 200 | |
| Berman (1990) | (1)* | −7548 | −56 572 | (A) |
| | | ±4730 | ±7 200 | |
| Berman (1990) | (3) | −5403 | −60 532 | (B) |
| | | ±4570 | ±6 970 | |

*Note:* All numbers are given in J/mol and are valid for Reaction 1. The standard state properties are taken from (1) Berman (1988, 1990); (2) biotite: Berman (1988, 1990), garnet: Berman and Aranovich (1996); (3) this study, derived by extrapolation of the partitioning data to annite (Fig. 15): $\Delta H^0_R = -50\,905$ J/mol, $\Delta S^0_R = -17.18$ J/(mol·K) and $\Delta V^0_R = -0.236$ J/mol from (Berman 1988, 1990); BA = Berman and Aranovich (1996); GS = Ganguly and Saxena (1984); HW = Hackler and Wood (1989). Italics represents preferred result. (A) and (B) denote results used for geothermometry, i.e., Equation 11 and 12.

* Berman (1988, 1990) valid for 600 to 800 °C and 2 kbar (see Fig. 15): $\Delta H^0_R = -57\,594$ J/mol, $\Delta S^0_R = -24.44$ J/(mol·K) and $\Delta V^0_R = -0.236$ J/mol.

though, a direct comparison is debatable because the data were fitted using different Al-biotite components.

Critically assessing the quality of the derived Margules parameters exhibits some limits: First, in particular the small range of Al contents in the biotites accounts for a large uncertainty of the computed $\Delta W_{Al}$ term. Second, omitted influences of $Fe^{3+}$ in biotite may be buried in the derived interaction parameters. Third, although the results presented here indicate that the annite standard state properties may need revision, they were used to perform the LSQ computations because of a lack of accurate, alternative data. Therefore, circularities may have been introduced. Nevertheless, the standard state properties of reaction derived by extrapolation allow a LSQ regression that is independent of these annite data and yields very similar biotite mixing properties to those obtained employing them (Table 4).

## Geothermometry and application

As a geothermometer, we suggest an expression disregarding heat capacity terms, which has, in contrast to Equation 5, the merit of easy application. Rearrangement of Equation 5 and omitting heat capacity terms gives

$$T(°C) = \{[\Delta H^0_R + (P - 1)\Delta V^0_R + \Delta G_{exc}] \div [\Delta S^0_R - 3R \ln K_D]\} - 273.15. \quad (9)$$

Insertion of the standard state thermodynamic properties and the formulation of adequate $\Delta G_{exc}$ term yields an expression that can be used as a geothermometer. Assuming an asymmetric mixing model for binary garnet and symmetric mixing in biotite (Eq. 8) gives:

$$\Delta G_{exc} = 3RT \ln K\gamma^{Gt} - 3RT \ln K\gamma^{Bio} = W^{Gt}_{MgFe}(X^{2Gt}_{Mg} - 2X^{Gt}_{Mg}X^{Gt}_{Fe}) + W^{Gt}_{FeMg}(2X^{Gt}_{Mg}X^{Gt}_{Fe} - X^{2Gt}_{Fe}) - W^{Bio}_{FeMg}(X^{Bio}_{Mg} - X^{Bio}_{Fe}) - (W^{Bio}_{FeAl} - W^{Bio}_{MgAl})X^{Bio}_{Al}. \quad (10)$$

On the basis of the LSQ regressions performed with the standard thermodynamic properties of reaction that are based on the data set of Berman (1988, 1990) for the *P-T* range of the experiments (see Fig. 15), the garnet activity model of Berman (1990), and assuming all Fe to be $Fe^{2+}$, insertion of Equation 10, with the respective interaction parameters [(A) in Table 4] into Equation 9, gives

$$T(°C) = \{[-57594 + 0.236(P - 1) + (230 + 0.01P) \times (X^{2Gt}_{Mg} - 2X^{Gt}_{Mg}X^{Gt}_{Fe}) + (3720 + 0.06P) \times (2X^{Gt}_{Mg}X^{Gt}_{Fe} - X^{2Gt}_{Fe}) - (-7548)(X^{Bio}_{Mg} - X^{Bio}_{Fe}) - (-56572)X^{Bio}_{Al}]/[-24.44 - 3R \ln K_D]\} - 273.15 \quad (11)$$

where

$$K_D = (X_{Fe}/X_{Mg})^{Gt}/(X_{Fe}/X_{Mg})^{Bio}.$$

A similar expression results with the standard state properties derived by extrapolation to annite (Fig. 15) and the respective Margules parameters [(B), Table 4]:

$$T(°C) = \{[-50905 + 0.236(P - 1) + (230 + 0.01P) \times (X^{2Gt}_{Mg} - 2X^{Gt}_{Mg}X^{Gt}_{Fe}) + (3720 + 0.06P) \times (2X^{Gt}_{Mg}X^{Gt}_{Fe} - X^{2Gt}_{Fe}) - (-5403)(X^{Bio}_{Mg} - X^{Bio}_{Fe}) - (-60532)X^{Bio}_{Al}]/[-17.18 - 3R \ln K_D]\} - 273.15. \quad (12)$$

These expressions are valid for assemblages with binary Fe-Mg garnets. For quaternary garnet compositions, an appropriate garnet activity model has to be inserted, introducing temperature-dependent terms (i.e., $W^{Gt}_s$ terms) on the right side of Equations 11 and 12, which then have to be rearranged to be solved for *T*.

The biotite compositions of selected studies are shown together with experimentally equilibrated biotite compositions in Figure 9, indicating significant amounts of vacancies for all biotite samples shown, except those herein. Extremely large deviations between reference temperatures and model temperatures (Eqs. 11 and 12) are obtained for assemblages with vacancy-bearing biotite samples (shown in Fig. 9) if the total amount of $^{[6]}Al$ in biotite is considered. However, the derived biotite-mixing properties are valid for Tschermak-substituted $^{[6]}Al$ according to the operational substitution, and much better *T* esti-

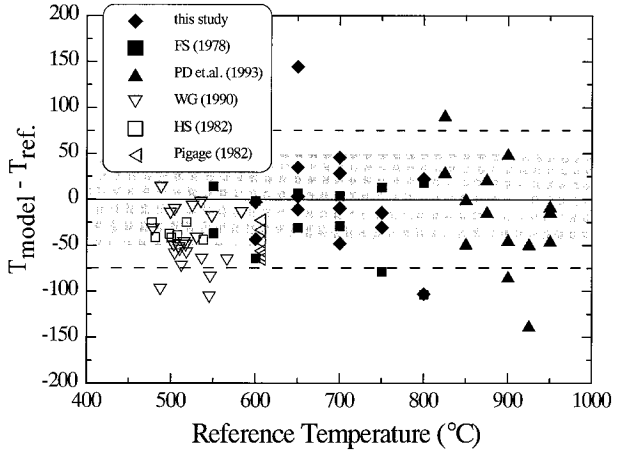


**FIGURE 16.** Deviations between temperature estimates ($T_{model}$) obtained with the presented garnet biotite geothermometer and reference temperatures as a function of the experimental and independently constrained temperatures. The shaded area indicates deviations of ±50 °C. (FS = Ferry and Spear 1978; PD et al. = Patino Douce et al. 1993; HS = Hodges and Spear 1982; WG = Williams and Grambling 1990). (FS = only $Alm_{90}Py_{10}$ experiments; the following samples have been taken from WG = Pecos Baldy 76-420, 77-125, 77-46D, 84-1632, 84-1631, 84-1622, 84-1621; Rio Mora 81-23a, 80-142, 80-46, C81-213, 81-13a, C81-310, 82-12; Cerro Colorado W84-35, W84-86, W84-94, W84-145, W85-195, W83-242, W84-133).

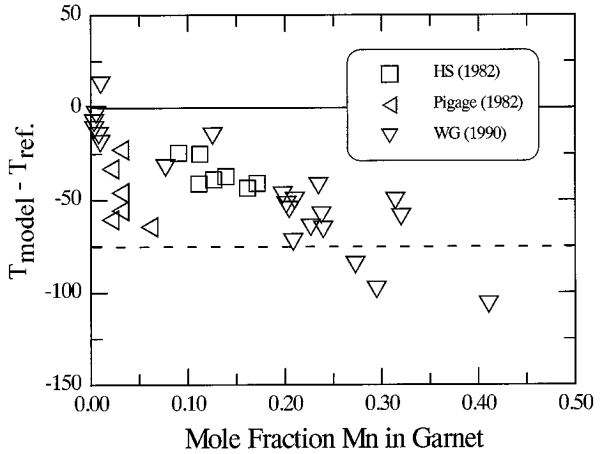


**FIGURE 17.** Temperature deviations ($T_{model} - T_{reference}$) as a function of garnet composition for the garnet-biotite assemblages reported by Hodges and Spear (1982), Pigage (1982), and Williams and Grambling (1990) showing increasing temperature deviations with increasing Mn content in garnet. Abbreviations as in Figure 16.

mates for both Equations 11 and 12 result if only that amount of $^{[6]}Al$ in the biotite of these assemblages is taken into account, which is balanced by Tschermak substitution (i.e., $^{[6]}Al_{Tsch}$ is defined as that amont of $^{[6]}Al$ that is balanced by $Al^{[4]}_{excess}$):

The application of Equation 12 to various garnet-biotite pairs is shown in Figure 16. The experimental temperatures of this study are reproduced to within ±50 °C (except two experiments for which tight brackets were not achieved; Table 2). The temperature estimates for the garnet-biotite pairs of Patino Douce and Johnston (1991) are mostly within ±50 °C of experimental temperatures (Fig. 16), although the biotite contains significant amounts of F ($X_F$ = 0.04–0.145) and Ti ($X_{Ti}$ = 0.07–0.12). The model temperatures for the garnet-biotite pairs of Ferry and Spear (1978), obtained with the recalculated Al-bearing biotite compositions (regression, Fig. 8) are also within ±50 °C of their experimental temperatures.

Temperature estimates obtained for natural garnet + biotite assemblages (Hodges and Spear 1982; Pigage 1982; Williams and Grambling 1990) are also shown in Figure 16. The Ti and F contents in the biotites of these studies are low, but the garnets contain considerable amounts of Ca and Mn. Therefore the quaternary garnet activity model of Berman (1990) was employed. The temperatures suggested by the authors were based on phase relations that imply *P-T* conditions close to the $Al_2SiO_5$ triple point. They are reproduced mostly within ±75 °C. A diagram (Fig. 17) showing the temperature deviations ($T_{model} - T_{reference}$) as a function of Mn content of garnet reveal increasing temperature deviations with increasing amount of spessartine component in garnet. This could be due to omitted compositional interdependencies or to an inadequate activity model for garnet.

The application of the derived Fe-Mg exchange geothermometer to experimental and natural samples from a wide *P-T* range reveals generally good temperature estimates if only Tschermak-substituted $^{[6]}Al$ is considered. Large temperature deviations have to be expected for parageneses that include garnet with high Mn contents. Remaining deviations between *T* estimates and reference temperatures may result from omitted heat capacity terms and from nonideal mixing effects of Ti, vacancies, and F in biotite.

## CONCLUDING REMARKS

The biotite samples in the study of Ferry and Spear (1978) have been generally treated as binary solid solutions, which is equivocal in the light of the present results. Their data with the assumption of strictly binary biotite compositions were employed, for instance, to derive biotite mixing properties (e.g., Kleemann and Reinhardt 1994) or to constrain the thermodynamic properties of annite (Berman 1990). The latter are part of a widely used thermodynamic data set (Berman 1988, 1990). It is obvious that the presented evidence for ternary biotite solid solutions in similar experiments may be of significance far beyond garnet-biotite thermometry.

## ACKNOWLEDGMENTS

We thank P. Drissen for performing the laser-granulation analysis and H. Ristedt and G. Oleschinski for support and technical assistance with the SEM observations. Many thanks are due to the members of the Mineralogical Institute at the University of Bonn for discussions, support, and technical help throughout the project. Comments and discussions by col-

leagues from the DFG (German research foundation) priority program ''Elementverteilung'' and from the Bayerisches Geoinstitute during the course of this work were greatly appreciated. Many thanks to S. Chakraborty, E. Dachs, C. Geiger, and A. Patino Douce for their careful reviews and constructive criticism that largely improved the manuscript. This study was made possible through a DFG grant (Sp 327/2).

## REFERENCES CITED

Benisek, A., Dachs, E., Redhammer, G., Tippelt, G., and Amthauer, G. (1996) Activity-composition relationship in Tschermak's substituted Fe biotites at 700°C, 2 kbar. Contributions to Mineralogy and Petrology, 125, 85–99.

Berman, R.G. (1988) Internally-consistent thermodynamic data for stoichiometric minerals in the system $Na_2O$-$K_2O$-CaO-MgO-FeO-$Fe_2O_3$-$Al_2O_3$-$SiO_2$-$TiO_2$-$H_2O$-$CO_2$. Journal of Petrology, 29, 445–522.

———(1990) Mixing properties of Ca-Mg-Fe-Mn garnets. American Mineralogist, 75, 328–344.

Berman, R.G. and Aranovich, L.Y. (1996) Optimized standard state and solution properties of minerals: I. Model calibration for olivine, orthopyroxen, cordierite, garnet and ilmenite in the system Fo-MgO-CaO-$Al_2O_3$-$TiO_2$-$SiO_2$. Contributions to Mineralogy and Petrology, 126, 1–24.

Bhattacharya, A., Mohanty, L., Maji, A., Sen, S.K., and Raith, M. (1992) Non-ideal mixing in the phlogopite-annite binary: constraints from experimental data on Mg-Fe partitioning and a reformulation of the biotite-garnet geothermometer. Contributions to Mineralogy and Petrology, 111, 87–93.

Brigatti, M.F., Galli, E., and Poppi, L. (1991) Effect of Ti substitution in biotite-1M crystal chemistry. American Mineralogist, 76, 1174–1183.

Chakraborty, S. and Ganguly, J. (1991) Compositional zoning and cation diffusion in garnets. In J. Ganguly, Ed., Diffusion, atomic ordering and mass transport, Advances in Physical Geochemistry, 8, p. 120–175. Springer Verlag, Berlin.

———(1992) Cation diffusion in aluminosilicate garnets: Experimental determination in spessartine-almandine diffusion couples, evaluation of effective binary diffusion coefficients, and applications. Contributions to Mineralogy and Petrology, 111, 74–86.

Chakraborty, S. and Rubie, D.C. (1996) Mg tracer diffusion in aluminosilicate garnets at 750–850 °C, 1 atm and 1300 °C, 8.5 GPa. Contributions to Mineralogy and Petrology, 122, 406–414.

Chatterjee, N. (1987) Evaluation of thermochemical data on Fe-Mg olivine, orthopyroxene, spinel and Ca-Fe-Mg-Al garnet. Geochimica et Cosmochimica Acta, 51, 2215–2226.

Circone, S. and Navrotsky, A. (1992) Substitution of $^{[6,4]}Al$ in phlogopite: High-temperature solution calorimetry, heat capacities, and thermodynamic properties of the phlogopite-eastonite join. American Mineralogist, 77, 1191–1205.

Crank, J. (1975) The mathematics of diffusion, 414 p. Oxford University Press, U.K.

Cygan, R.T. and Lasaga, A.C. (1985) Self-diffusion of magnesium in garnet at 750 °C to 900 °C. American Journal of Science, 285, 328–350.

Dachs, E. (1994) Uncertainties in the activities of garnets and their propagation into geothermobarometry. European Journal of Mineralogy, 6, 291–295.

Dallmeyer, R.D. (1974) The role of crystal structure in controlling the partitioning of Mg and $Fe^{2+}$ between coexisting garnet and biotite. American Mineralogist, 59, 201–203.

Dasgupta, S., Sengupta, P., Guha, D., and Fukuoka, M. (1991) A refined garnet-biotite Fe-Mg exchange geothermometer and its application in amphibolites and granulites. Contributions to Mineralogy and Petrology, 109, 130–137.

Deming, W.E. (1943) Statistical adjustment of data. Wiley, New York.

Dowty, E. (1980) Crystal-chemical factors affecting the mobility of ions in minerals. American Mineralogist, 65, 174–182.

Eckert, J.O. and Bohlen, S.R. (1992) Reversed experimental determination of the Mg-$Fe^{2+}$ exchange equilibrium in Fe-rich garnet-orthopyroxene pairs. Eos, 73, 608.

Eugster, H.P. (1957) Heterogeneous reactions involving oxidation and reduction at high pressures and temperatures. Journal of Chemistry and Physics, 26, 1760 p.

Eugster, H.P. and Wones, D.R. (1962) Stability relations of the ferruginous biotite, annite. Journal of Petrology, 3, 82–125.

Ferry, J.M. and Spear, F.S. (1978) Experimental calibration of the partitioning of Fe and Mg between biotite and garnet. Contributions to Mineralogy and Petrology, 66, 113–117.

Forbes, W.C. and Flower, M.F.J. (1974) Phase relations of titanphlogopite, $K_2Mg_4TiAl_2Si_6O_{20}(OH)_4$: a refractory phase in the upper mantle? Earth and Planetary Science Letters, 22, 60–66.

Frentrup, K.R. (1980) Absorptionsspektren von synthetischen Silikatgranaten und Granatmischkristallen und ihre Anwendung zur spektroskopischen 3d-Ionenanalyse in Granaten. unpublished Dissertation, Universität Bonn, 216 p.

Fritz, S.F. and Popp, R.K. (1985) A single-dissolution technique for determining FeO and $Fe_2O_3$ in rock and mineral samples. American Mineralogist, 70, 961–968.

Ganguly, J. (1978) Energetics of some ferromagnesian silicate solid solutions derived from compositional relations between coexisting phases. Physics and Chemistry of Minerals, 3, 301–302.

Ganguly, J. and Saxena, S.K. (1984) Mixing properties of aluminosilicate garnets: constraints from natural and experimental data, and applications to geothermo-barometry. American Mineralogist, 69, 88–97.

———(1987) Mixtures and Mineral reactions, 291 p. Springer Verlag, New York.

Ganguly, J. Cheng, W., and Tirone, M. (1996) Thermodynamics of aluminosilicate garnet solid solution: new experimental data, an opitmized model, and thermometric applications. Contributions to Mineralogy and Petrology, 126, 131–151.

Geiger, C.A. and Rossman, G.R. (1994) Crystal field stabilization energies of almandine-pyrope and almandine-spessartine garnets determined by FTIR near infrared measurements. Physics and Chemistry of Minerals, 21, 516–525.

Geiger, C.A., Newton, R.C., and Kleppa, O.J. (1987) Enthalpy of mixing of synthetic almandine-grossular and almandine-pyrope garnets from high-temperature solution calorimetry. Geochimica et Cosmochimica Acta, 51, 1755–1763.

Gessmann, C.K. (1995) Experimentelle Untersuchung der Effekte von Titan und $Aluminium^{VI}$ im Biotit auf den Fe-Mg-Austausch zwischen Granat und Biotit. Bonner Geowissenschaftliche Schriften, 17, Bonn, Holos Verlag, 125 p.

Gessmann, C., Spiering, B., and Raith, M. (1994) Experimental investigation of the Fe-Mg-partitioning between garnet and biotite with respect to the influence of Ti in biotite. Mineralogical Magazine, 58A, 327–328.

Giletti, B.J. (1985) The nature of oxygen transport within minerals in the presence of hydrothermal water and the role of diffusion. Chemical Geology, 53, 197–206.

Goldman, D.S. and Albee, A.L. (1977) Correlation of Mg/Fe partitioning between garnet and biotite with $^{18}O/^{16}O$ partitioning between quartz and magnetite. American Journal of Science, 277, 750–767.

Hackler, R.T. and Wood, B.J. (1989) Experimental determination of Fe and Mg exchange between garnet and olivine and estimation of Fe-Mg mixing properties in garnet. American Mineralogist, 74, 994–999.

Hodges, K.F. and McKenna, L.W. (1987) Realistic propagation of uncertainties in geologic thermobarometry. American Mineralogist, 72, 671–680.

Hodges, K.V. and Spear, F.S. (1982) Geothermometry, geobarometry and the $Al_2SiO_5$ triple point at Mt. Moosilauke, New Hampshire, American Mineralogist, 67, 1118–1134.

Hoisch, T.D. (1991) Equilibria within the mineral assemblage quartz + muscovite + biotite + garnet + plagioclase, and implications for the mixing properties of octahedrally coordinated cations in muscovite and biotite. Contributions to Mineralogy and Petrology, 108, 43–54.

Indares, A. and Martignole, J. (1985) Biotite-garnet geothermometry in the granulite facies: the influence of Ti and Al in biotite. American Mineralogist, 70, 272–278.

Keesmann, I., Matthes, S., Schreyer, W., and Seifert, F. (1971) Stability of almandine in the system FeO-($Fe_2O_3$)-$Al_2O_3$-$SiO_2$-($H_2O$) at elevated pressures. Contributions to Mineralogy and Petrology, 31, 132–144.

Kleemann, U. and Reinhardt, J. (1994) Garnet-biotite thermometry revis-

ited: The effect of $Al^{VI}$ and Ti in biotite. European Journal of Mineralogy, 6, 925–941.

Koziol, A.M. and Bohlen, S.R. (1992) Solution properties of almandine-pyrope garnet as determined by phase equilibrium experiments. American Mineralogist, 77, 765–773.

Lee, H.Y. and Ganguly, J. (1988) Equilibrium compositions of coexisting garnet and orthopyroxene: Experimental determinations in the system FeO-MgO-$Al_2O$-$SiO_2$, and applications. Journal of Petrology, 29, 99–113.

Mueller, R.F. (1972) Stability of biotite: A discussion. American Mineralogist, 57, 300–316.

Munoz, J.L. (1984) F-OH and Cl-OH exchange in micas with applications to hydrothermal ore deposits. In Mineralogical Society of America Reviews in Mineralogy, 13, 469–491.

Newton, R.C. and Haselton, H.T. (1981) Thermodynamics of the garnet-plagioclase-$Al_2SiO_5$-quartz geobarometer. In R.C. Newton, A. Navrotsky, and B.J. Wood, Eds., Thermodynamics of minerals and melts, Advances in Physical Geochemistry, 2, p. 129–145. Springer Verlag, New York.

Patiño Douce, A.E. and Johnston, A.D. (1991) Phase equilibria and melt productivity in the pelitic system: implications for the origin of peraluminous granitoids and aluminous granulites. Contributions to Mineralogy and Petrology, 107, 202–218.

Patiño Douce, A.E., Johnston, A.D., and Rice, J.M. (1993) Octahedral Excess mixing properties in biotite: A working model with applications to geobarometry and geothermometry. American Mineralogist, 78, 113–131.

Pattison, D.R.M. (1994) Are reversed Fe-Mg exchange and solid solution experiments really reversed? American Mineralogist, 79, 938–950.

Pattison, D.R.M. and Newton, R.C. (1989) Reversed experimental calibration of the garnet-clinopyroxene Fe-Mg-exchange thermometer. Contributions to Mineralogy and Petrology, 75, 87–103.

Perchuk, L.L. and Lavrent'eva, I.V. (1983) Experimental investigation of exchange equilibria in the system cordierite-garnet-biotite. In S.K. Saxena, Ed., Kinetics and equilibrium in mineral reactions, p. 199–239. Springer Verlag, New York.

Perchuk, L.L., Aranovich, L.Y., Podlesskii, K.K., Lavrent'eva, I.V., Gerasimov, V.Y., Fed'kin, V.V., Kitsul, V.I., Karsakov, L.P., and Berdnikov, N.V. (1985) Precambrian granulites of the Aldan shield, Eastern Siberia, USSR. Journal of metamorphic Geology, 3, 265–310.

Perkins III, D., Holland, T.J.B., and Newton, R.C. (1981) The $Al_2O_3$ contents of enstatite in equilibrium with garnet in the system MgO-$Al_2O_3$-$SiO_2$ at 15–40 kbar and 900–1600 °C. Contributions to Mineralogy and Petrology, 78, 99–109.

Peterson, J.W., Chacko, T., and Kuehner, S.M. (1991) The effects of fluorine on the vapor-absent melting of phlogopite + quartz: Implications for deep-crustal processes. American Mineralogist, 76, 470–476.

Pigage, L.C. (1982) Linear regression analysis of sillimanite-forming reactions at Azure Lake, British Columbia. Canadian Mineralogist, 20, 349–378.

Pouchou, J.L. and Pichoir, F. (1984) A new model for quantitative x-ray microanalysis, part I: Application to the analysis of homogeneous samples. La Recherche Aerospace, 3, 167–192.

Redhammer, G.J., Dachs, E., and Amthauer, G. (1995) Mössbauer spectroscopic and X-ray powder diffraction studies of synthetic micas on the join Annite $KFe_3AlSi_3O_{10}(OH)_2$-Phlogopite $KMg_3AlSi_3O_{10}(OH)_2$. Physics and Chemistry of Minerals, 22, 282–294.

Rudert, V., Chou, I.-M., and Eugster, H.P. (1976) Temperature gradients in rapid-quench cold-seal pressure vessels. American Mineralogist, 61, 1012–1015.

Rutherford, M.J. (1973) The phase relations of aluminous biotites in the system $AlSi_3O_8$-$KAlSiO_4$-$Al_2O_3$-Fe-O-H. Journal of Petrology, 14, 159–180.

Saxena, S.K. (1969) Silicate solid-solution and geothermometry. 3-Distribution of Fe and Mg between coexisting garnet and biotite. Contributions to Mineralogy and Petrology, 22, 259–267.

Schulien, S. (1975) Determination of the equilibrium constant and the enthalpy of the reaction for the $Mg^{2+}$-$Fe^{2+}$ exchange between biotite and a salt solution. Fortschritte der Mineralogie, 52, 133–139.

Sengupta, P., Dasgupta, S., Bhattacharya, P.K., and Mukherjee, M. (1990) An orthopyroxene-biotite geothermometer and its application in crustal granulites and mantle-derived rocks. Journal of metamorphic Geology, 8, 191–197.

Shannon, R.D. and Prewitt, C.T. (1969) Effective ionic radii in oxides and fluorides. Acta Crystallographica, B 25, 925–946.

Spear, F.S. (1994) Metamorphic phase equilibria and pressure-temperature-time paths, 799 p. Mineralogical Society of America Monograph Series, Washington, D.C.

Spiering, B. (1982) Oxidationszustand und Koordination des Eisens in granitischen Schmelzen und Gesteinen. Ph.D. Dissertation, Universität Kiel, 147 p.

Thompson, A.B. (1976) Mineral reactions in pelitic rocks: II. Calculation of some P-T-X(Fe-Mg) phase relations. American Journal of Science, 276, 425–454.

Williams, M.L. and Grambling, J.A. (1990) Manganese, ferric iron, and the equilibrium between garnet and biotite. American Mineralogist, 75, 886–908.

Wones, D.R. (1963) Physical properties of synthetic biotites on the join phlogopite-annite. American Mineralogist, 48, 1300–1321.

———(1972) Stability of biotite: A reply. American Mineralogist, 57, 316–317.

Wones, D.R. and Eugster, H.P. (1965) Stability of biotite: experiment, theory, and application. American Mineralogist, 50, 1228–1272.

Woodland, A.B. and Wood, B.J. (1989) Electrochemical measurement of the free energy of almandine ($Fe_3Al_2Si_3O_{12}$) garnet. Geochimica et Cosmochimica Acta, 53, 2277–2282.

Manuscript received January 9, 1996
Manuscript accepted July 2, 1997